# Chapter 6

# Thermodynamic Analysis of 660 MW Supercritical Power Plant Retrofitted to Oxy-coal combustion

## 6.1 Overview

This chapter presents thermodynamic analysis of 660 MW pulverized coal fired power plant retrofitted to oxy-coal combustion. Oxy-coal combustion power plant comprises of air separation unit (ASU), oxy-coal combustion unit, steam cycle and $CO_2$ compression and purification unit (CPU). Incorporation of ASU and CPU in power generation system reduces net plant efficiency as these units consume sufficient power. Advantage of retrofitting conventional air-fired power plant to work under oxy-coal is observed in term of high $CO_2$ recovery and high $CO_2$ purity.

## 6.2 Assumptions and Modelling Approach

There are four subsystems of analysed oxy-coal fired supercritical steam power plant: boiler island, supercritical steam cycle, ASU and CPU units. The developed steady state model in Aspen Plus (V10.0) is based on the following assumptions: (1) Cryogenic ASU was employed for the required oxygen supply to the oxy-coal boiler. (2) The macro thermodynamic feature of complex combustion was considered through the simplified furnace model. (3) The high temperature flue gas produced after combustion was flown through the heat transfer sections of the boiler to change the state of feedwater into steam. (4) The 95% pure oxygen stream supplied to boiler is mixed with recycled flue gas (around 70% of total flue gas produced) and sent to the oxy-coal burner. (5) The oxygen concentration is maintained at 25 vol % in recycle flue gas (RFG) and oxygen mixture. (6) Ambient temperature ($T_0$) and pressure ($P_0$) of the reference atmosphere were considered as 33℃ and 1.013 bar. (7) The terminal temperature difference (TTD), defined as the difference between bleed steam saturation temperature and feed water exit temperature of HP and LP FWHs was assumed as 0℃ and 3℃, respectively. (8) 2% air ingress into the furnace was assumed.

In the initial step, a supercritical power plant configuration is transformed into a process flow diagram, with input from different sources including scientific literatures. A process flow diagram is then used to generate thermodynamic material and energy balance on process simulation tool Aspen plus. This will form the basis for thermodynamic performance analysis.

**Table 6.1** Characteristics of pulverized coal (Naidu et al., 2016)

| **Proximate analysis (as received wt.%)** | | **Ultimate analysis (dry basis wt.%)** | |
|---|---|---|---|
| Moisture | 12 | Carbon (C) | 39.16 |
| Ash | 43 | Hydrogen (H) | 2.76 |
| Volatile matter | 21 | Nitrogen (N) | 0.78 |
| Fixed carbon | 24 | Sulphur (s) | 0.51 |
| HHV (MJ/kg) | 11.73 | Oxygen (O) | 7.92 |
| | | Ash | 48.87 |

Table 6.1 summarizes the characteristics of pulverized coal used as fuel in the present study. The coal has higher ash content usually employed for power generation under Indian climatic conditions. The composition of ash (in wt% dry basis) is assumed as $Al_2O_3$: 13.13, $SiO_2$: 32.68 and $Fe_2O_3$: 4.72. The following two cases are considered in the present study:

- A supercritical power plant working under conventional air-fired pulverized coal combustion without $CO_2$ capture (schematic diagram is shown in Fig. 6.1).
- A supercritical power plant working under oxy-fuel combustion condition with consideration of $CO_2$ capture (schematic diagram is shown in Fig. 6.2).

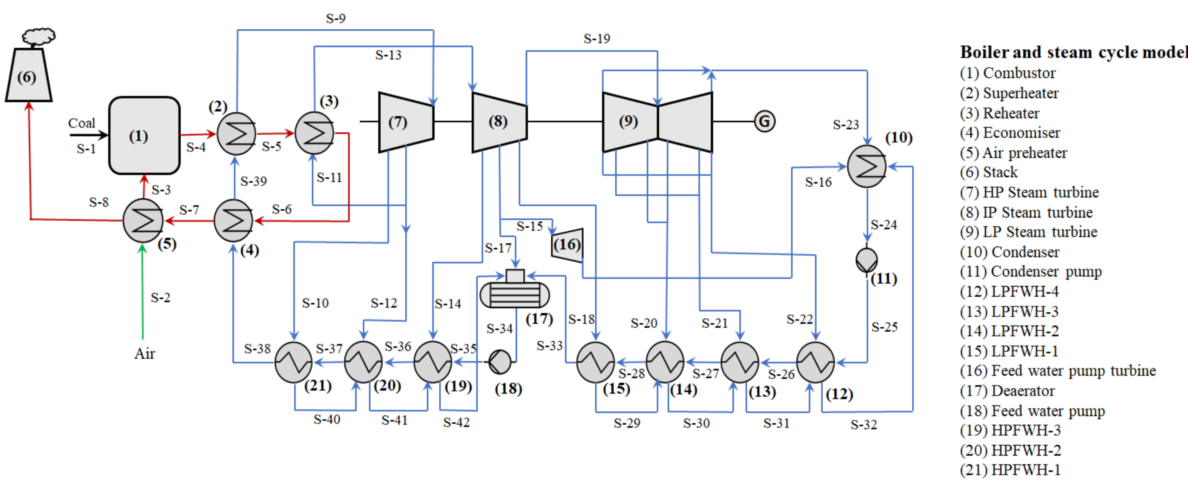


**Fig. 6.1.** Schematic diagram of 660 MW supercritical power plant working under conventional air-fired pulverized coal combustion without $CO_2$ capture

## 6.3 Air Separation Unit (ASU) Modelling

Air separation unit (ASU) consumes substantial amount of power of oxy-coal combustion steam power plant. The present work employs two column cryogenic distillation-based ASU for oxygen production. At present, the cryogenic ASU is the only technology capable of guaranteeing required volume and purity of $O_2$ for the larger-scale boilers. The major drawback of this oxygen production technology is its high energy demand, which amounts to 0.22-0.24 kWh/kg$O_2$ at a purity of 95% (Skorek-Osikowska et al., 2015). ASU consists of a multi-stage compressor, heat exchanger, expansion valve and distillation column. The compressed air fed to the multi-stage compressor at atmospheric temperature and pressure is the driving power of the separation process. For the simplified calculations, the composition of air is assumed to be 20.9% oxygen and 78.2% nitrogen and 0.9% argon.

The schematic of air separation unit is shown in Fig. 6.2 (a). In the first step, air is compressed in four stage compressor with intersectional cooling down to 30℃ and 6.3 bar. Constant pressure ratio was maintained for each stage. After compression, air is cooled in multi-stream heat exchanger. Liquified air entering the distillation column is separated into liquid $O_2$ as bottom product and vapor $N_2$ as top product. Both top and bottom products have some impurities. Main operation parameters of ASU are given in Table 6.2.

**Table 6.2** Main operation parameters of the ASU installation

| **Parameter** | **Unit** | **Value** |
|---|---|---|
| Air temperature at inlet to ASU installation | ℃ | 33 |
| Air pressure at inlet to ASU installation | bar | 1.013 |
| Air supplied to ASU | Kg/s | 608.1 |
| Percentage of nitrogen in air | % | 78.2 |
| Percentage of oxygen in air | % | 20.9 |
| Air temperature at the outlet of the intersectional coolers | ℃ | 30 |
| Pressure in the high-pressure column | bar | 6.3 |
| Pressure in the low-pressure column | bar | 1.3 |
| Purity of separated oxygen | % | 95 |
| Isentropic efficiency of air compressor | - | 0.85 |
| Mechanical efficiency of air compressor | - | 0.98 |

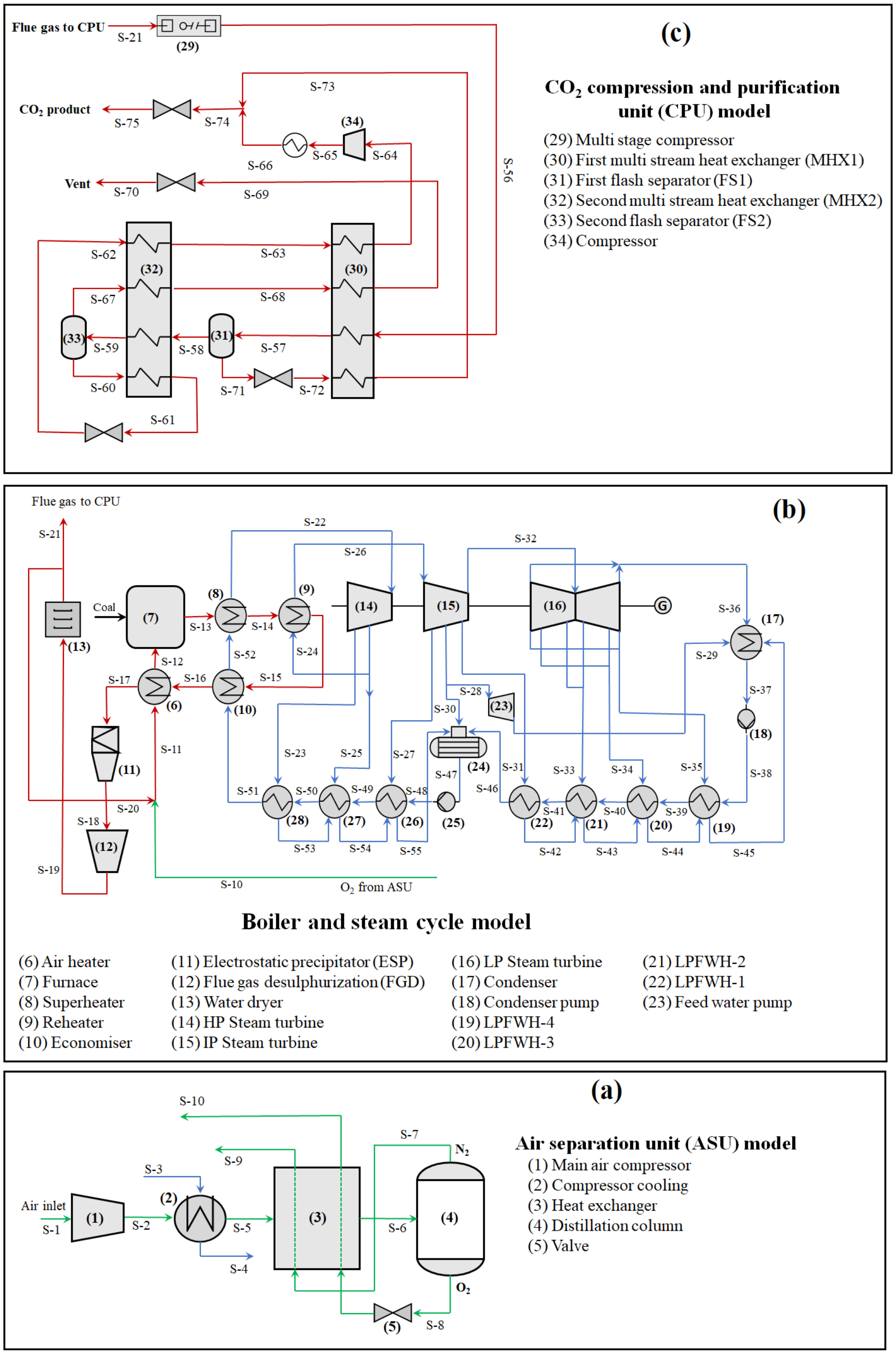


**Fig. 6.2.** Schematic of 660 MW power plant comprising of **(a)** ASU **(b)** supercritical Rankine cycle and **(c)** CPU retrofitted to oxy-fuel combustion

## 6.4 Description of Model for Oxy-Coal Combustion

The coal combustion phenomenon under oxy-fuel combustion atmosphere takes place under following assumptions: (1) The pulverized coal combustion process under oxy-fuel atmosphere has four sequential stages: drying, devolatilization, combustion and the removal of flue gas dust. (2) Stable and time independent operation of the blocks are assumed. (3) Homogeneous mixing of pulverized coal and air takes place in the reactor. (4) The coal pyrolysis vaporises the constituents of coal O, N, H and S into the gaseous phase, whereas element C is transformed into pure coke. Ash doesn't participate in the reaction during PC combustion.

Fig. 6.3 displays the flowsheet of oxy-coal combustion. In the first step, drying block (RStoic) reduces the moisture level of wet coal from 12% to 2%. Flashing block (FLASH2) evaporates remaining traces of $H_2O$. Pyrolysis of completely dry pulverized coal takes place in decomposition block (RYield). The products of the pyrolysis are analysed by calculator block. The combustion process is simulated by Gibbs reactor (RGibbs).

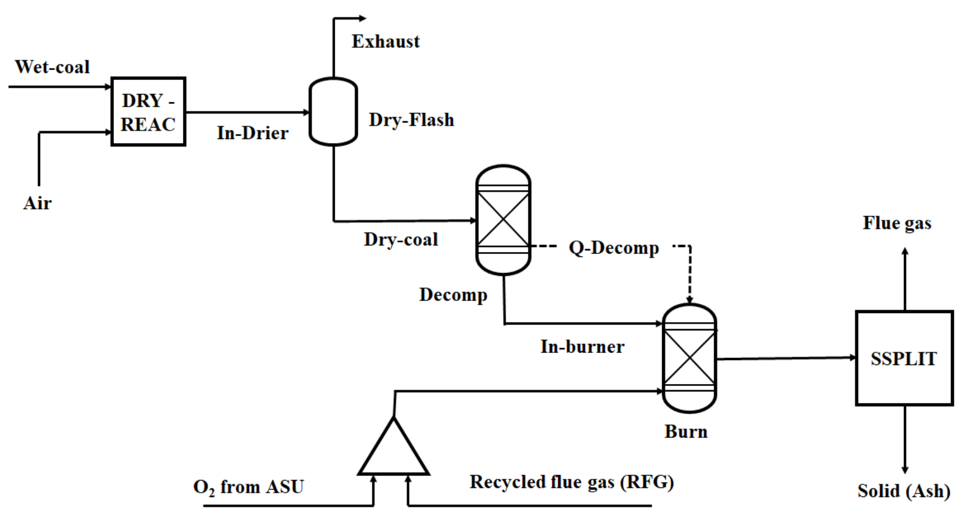


**Fig. 6.3.** Flowsheet of oxy-coal combustion of pulverized coal

**Table 6.3** Essential input parameters for oxy-fuel combustion

| | Wet coal | Air supplied to dry reactor | Oxidizer supplied for combustion |
|---|---|---|---|
| Temperature (℃) | 33 | 300 | 350 |
| Pressure (bar) | 1.03 | 1.03 | 1.03 |
| Mass flow rate (kg/s) | 102.9 | 200 | 499.832 |
| Composition | - | 21% $O_2$ + 79% $N_2$ | 25% $O_2$ +RFG |

The combustion process is simulated by Gibbs reactor (RGibbs). In the Gibbs reactor, the mixture of recycled flue gas (RFG) and $O_2$ are employed as oxidizer. At the minimum value of Gibbs free energy, chemical reaction finishes completely. The separation of ash from the flue gases takes place in the separation block (SSplit). Around 70% of the total flue gas produced is recycled to mix with $O_2$ and supplied to RGibbs. Remaining flue gas is allowed to flow through the heat transfer sections of boiler to change the state of feed water into steam. The essential input parameters of oxy-coal combustion are given in Table 6.3.

### 6.4.1 Coal Drying Unit

Coal dying is modelled in RStoic block according to Eq. (6.1). Drying unit reduces moisture level from 12% to 2% with the help of Fortran calculator block.

$$COAL(wet) \rightarrow 0.0555084 H_2O + COAL(dry) \tag{6.1}$$

### 6.4.2 Decomposition Unit

Pulverized coal is decomposed into its constituents and ash in RYield block. During the decomposition the heat released is sent to RGibbs for combustion. Fortran block calculates the decomposition products and ash. The enthalpy balance equation of unit is given in Eq$^n$. (6.2).

$$\sum_{i=1}^{I} m_i \Delta H^0_{f,i,298} + \sum_{i=1}^{I} m_i \int_{298}^{T} c_{p,T.i} dT = \sum_{j=1}^{J} n_j \Delta H^0_{f,i,298} + \sum_{j=1}^{J} n_j \int_{298}^{T} c_{p,T.i} dT + Q_P \tag{6.2}$$

### 6.4.3 Burn Unit

The phase and chemical equilibrium of the chemical reactions are modelled by RGibbs unit through the minimization of the system's Gibbs free energy (Pei et al., 2013). $CO_2$, CO, $H_2O$, $N_2$, $SO_2$, $SO_3$, NO, $NO_2$ and ash are main combustion products. The mathematical model for Gibbs free energy minimization is shown below

$$MinG, G = \sum_{j=1}^{s} n_j^c G_J^0 + \sum_{j=s+1}^{M} \sum_{l=1}^{P} n_{jl} G_{jl} \tag{6.3}$$

Where G is system's Gibbs free energy. S, M and P represent single phase, number of phases and components, respectively.

## 6.5 Description of Model for Steam Cycle

The oxy-coal combustion system analysed in this study is a 660 MW supercritical plant that includes boiler, turbines and feedwater heaters, high-pressure turbine (HPT), intermediate pressure turbine (IPT) and low-pressure turbines (LPT) shown in Fig. 6.2(b). The live steam (S-22) is supplied to the HPT at 537°C temperature and 242.2 bar pressure. The pressure and temperature of reheated steam (S-26) supplied to IPT are 42.40 bar and 565°C. After the turbine expansion is completed, steam (92.60% quality) enters the steam condenser operating at 0.103 bar pressure. Cooling water fed to the water-cooled condenser at 33℃, gains 10℃ temperature in the condenser. Four low-pressure feedwater heaters (LPFWH) and three high-pressure feedwater heaters (HPFWH) heat the condensate leaving the condenser.

**Table 6.4** Steam cycle parameters of the 660 MW Super critical power plant

| | **Super critical parameters** | | | |
|---|---|---|---|---|
| | **P (bar)** | **T(℃)** | **Steam mass flow rate (kg/s)** | **Isentropic efficiency (%)** |
| HP Turbine inlet | 242.2 | 537 | 550.7 | 89.6 |
| IP Turbine inlet | 42.0 | 565 | 466.2 | 91.7 |
| LP Turbine inlet | 2.9 | 215.6 | 173.0 | 85.7 |
| Steam quality (at LPT exhaust) | 0.93 | | | |
| Condenser pressure (kPa) | 10.3 | | | |

Open-contact heat exchanger (OCFWH) working as deaerator at 21 bar pressure**,** a condensate pump, a main feedwater pump (FWP) and a circulating pump are also included in the steam cycle. The present study assumes TTD in high pressure and low-pressure regenerative heat exchanger as 0℃ and 3℃, respectively. The essential input parameters for 660 MW supercritical power plant is given in Table 6.4.

## 6.6 Description of Model for $CO_2$ Compression and Purification Unit

Fig. 6.2 (c) displays the schematic diagram of the CPU. The design of CPU has been adopted from optimized study of Jin et al. (2015a). They have performed multivariable optimization of CPU to achieve the best possible operating conditions and establish reliable control of desirable operations. The CPU unit consists mainly of multi-stage $CO_2$ compressor (MCC), two multi steam heat exchangers, two flash separators, compressor, valves and cooler. The flue gas fed to the multi-stage compressor is compressed to 30 bar. The impurities of the compressed flue gas are removed in the cold box mainly consisting of two multi-stream heat exchangers (MHX) and two flash separators. The first multi-stream heat exchangers (MHX1) cool downs flue gas to -24.64℃, then it enters in flash separator 1 (FS1). The bottom product of FS1 is liquid $CO_2$, the top product is further cooled down in MHX2 to -55℃. Then the flue gas is fed to FS2, where bottom stream provides $CO_2$ product and the top stream is vent gas. At last, the second $CO_2$ products are mixed with the first $CO_2$ products for storage or utilization.

## 6.7 Methodologies

The thermodynamic calculations are based on the steady-state assumption. Each component of the schematic diagram Fig. 6.1-6.3 is control volume. Each block is in equilibrium of mass and energy.

$$\sum \dot{m}_{in} = \sum \dot{m}_{out} \tag{6.4}$$

$$\dot{Q} - \dot{W} = \sum \dot{m}_{in} h_{in} - \sum \dot{m}_{out} h_{out} \tag{6.5}$$

The net efficiency of plant power $\eta_{net}$, %, is defined as:

$$\eta_{net} = \frac{W_{net}}{Q_s} \times 100\% \tag{6.6}$$

Where $Q_s$ and $W_{net}$ represent heat supplied and the net power output.

Net power output is estimated as follows:

$$W_{net} = W_{st} - \sum W_{aux,i} \tag{6.7}$$

$W_{st}$ is the steam turbine power output; $\sum W_{aux,i}$ are the auxiliary power consumption of technical installations of oxy-coal combustion system. These auxiliary-power consuming technical installations include ASU, steam boiler island and steam cycle and CPU unit.

Aspen Plus (V 10.0) has been used to develop the steady-state model of power plants configurations. Aspen plus consists of integrated programs capable of easily assembling the energy generation plants from various energy component modules. Thermodynamically rigorous material and energy balance have been established on process flow diagrams employing this kind of process simulation tools. The present work primarily consists of models for turbines/compressors, heat exchangers, pumps, separators and reactors. Compressors/turbines and pumps use Compr and Pump blocks for expansion and pressurization of gases or fluids. HeatX block has been employed for modelling of heat exchangers. RYield and RGibbs blocks have been combined for describing the combustion reactions in the furnace. The properties have been satisfactory calculated by employing the PRBM method.

## 6.8 Validation

The validation of simulation results obtained by employing process simulation tool Aspen plus for 660 MW pulverized coal-fired supercritical power plant has been presented in Table 6.5. The corresponding stream number given in Table 6.5, can be seen in the schematic diagram of the conventional air-fired power plant shown in Fig. 6.1. The operational values of the supercritical power plant have been taken from the work of Suresh et al. (2010). From Table 6.5, it can be seen that the stream flow data values are close to the corresponding operational values having a maximum deviation below 5%.

**Table 6.5** Validation of stream data of 660 MW supercritical power plant (corresponding stream numbers can be seen in Fig. 6.1)

| | | Temperature (°C) | | | Mass flow rate (kg/s) | | |
|---|---|---|---|---|---|---|---|
| **Stream no.** | **Pressure (bar)** | **Operation** | **Simulation** | **% Variation** | **Operation** | **Simulation** | **% Variation** |
| S-1 | 1.030 | 33 | 33 | 0 | 102.9 | 102.9 | 0 |
| S-2 | 1.013 | 33 | 33 | 0 | 608.1 | 608.1 | 0 |
| S-3 | 1.030 | 272.1 | 272.3 | +0.0735 | 608.1 | 608.1 | 0 |
| S-4 | 1.010 | 1771.9 | 1798.63 | +1.5 | 700.9 | 700.5 | -0.057 |
| S-5 | 1.005 | 905.2 | 897.84 | -0.813 | 700.9 | 700.5 | -0.057 |
| S-6 | 1.005 | 542.4 | 535.009 | -1.36 | 700.9 | 700.5 | -0.057 |
| S-7 | 1.000 | 319 | 313 | -1.88 | 700.9 | 700.5 | -0.057 |
| S-8 | 1.060 | 130 | 128.321 | -1.29 | 700.9 | 700.5 | -0.057 |
| S-9 | 242.2 | 537 | 537 | 0 | 550.7 | 550.7 | 0 |
| S-10 | 66.8 | 340 | 332.85 | -2.1 | 36.2 | 36.2 | 0 |
| S-11 | 44.3 | 288.7 | 275.857 | -4.44 | 466.2 | 466.2 | 0 |
| S-12 | 44.3 | 288.7 | 275.857 | -4.44 | 48.3 | 48.3 | 0 |
| S-13 | 42 | 565 | 565 | 0 | 466.2 | 466.2 | 0 |
| S-14 | 21 | 459.9 | 442.85 | -3.70 | 14.4 | 14.4 | 0 |
| S-17 | 11.9 | 381.1 | 372.495 | -2.31 | 22.4 | 22.4 | 0 |
| S-18 | 6.1 | 295.4 | 286.767 | -2.92 | 19.2 | 19.1942 | -0.030 |
| S-19 | 2.9 | 215.6 | 206.767 | -4.09 | 173 | 173 | 0 |
| S-20 | 2.98 | 215.6 | 206.767 | -4.09 | 31.4 | 31.292 | -0.344 |
| S-21 | 0.64 | 87.6 | 89.7497 | +2.45 | 14.1 | 14.1485 | +0.344 |
| S-22 | 0.27 | 66.7 | 69.2461 | +3.81 | 13.5 | 13.4297 | -0.520 |

| | | | | | | | |
|---|---|---|---|---|---|---|---|
| S-23 | 0.103 | 46.4 | 48.3095 | +4.11 | 318.5 | 319.6 | +0.345 |
| S-24 | 0.103 | 46.4 | 48.3095 | +4.11 | 429.5 | 430.15 | +0.1513 |
| S-25 | 11.9 | 46.5 | 48.3834 | +4.05 | 429.5 | 430.15 | +0.1513 |
| S-35 | 308.7 | 193.9 | 187.717 | -3.188 | 550.7 | 550.7 | 0 |
| S-38 | 308.7 | 279.6 | 272.733 | -2.456 | 550.7 | 550.7 | 0 |
| S-39 | 308.7 | 341 | 341 | 0 | 550.7 | 550.7 | 0 |

## 6.9 Results of Thermodynamic Analysis

**Table 6.6** Summary of thermodynamic performance

| **Parameter** | | **Conventional combustion** | **Oxy-fuel combustion** |
|---|---|---|---|
| Air separation unit (ASU) | | | |
| Oxygen purity | mol% | - | 95.00 |
| Oxygen produced | kg/s | - | 108.287 |
| Specific power consumption | kW.hr/tonne | - | 295.85 |
| Power consumption | MW | - | 115.296 |
| $CO_2$ compression and purification unit (CPU) | | | |
| Power consumption | MW | | 42.512 |
| Specific power consumption | kW.hr/tonne | - | 97.552 |
| Miscellaneous power consumption | | | |
| Condensate pump | MW | 1.6234 | 1.6234 |
| Boiler feed water pump | MW | 30.7348 | 30.7348 |
| Net power consumption | MW | 32.3534 | 190.1662 |
| $CO_2$ purity | mol% | 13.15 | 95 |
| $CO_2$ recovery | % | - | 96 |
| Gross power output | MW | 692.523 | 692.523 |
| Heat supplied | MW | 1518.726 | 1518.726 |
| Net power output | MW | 660.1696 | 502.3568 |
| Gross efficiency | % | 45.60 | 45.60 |
| Net efficiency | % | 43.47 | 33.07 |

Table 6.6 displays the summary of thermodynamic performance of both convention air fired and oxy-coal fired supercritical power plant. The mole fraction of $O_2$ in the oxidizer is maintained at 25% with the help of design specification block for oxy-fuel combustion case at recycle ratio of 0.7. The oxy-fuel combustion power generation case has 10.4% reduction in net efficiency due to incorporation of ASU and CPU. Oxy-coal combustion power generation case is able to capture carbon dioxide with 95% purity and 96% recovery rate.

## 6.10 Results of Sensitivity Analysis

### 6.10.1 Influence of Oxygen Concentration in the Oxidizer

This section insight the influence of the concentration of oxygen on the composition of the flue gas produced in oxy-coal combustion atmosphere. To access the influence of oxygen concentration, the recycle ratio is fixed at 0.7.

Fig. 6.4-6.6 displays the influence of oxygen mole fraction in oxidizer on the composition of flue gas produced under oxy-fuel combustion condition. With an increase in oxygen concentration, the amounts of $CO_2$, $NO_x$ and $SO_3$ increases in the flue gas. Increase in oxygen concentration decreases the amounts of CO and $N_2$, whereas the mass flow rate of $SO_2$ increases initially up to oxygen concentration 24% and after that start decreasing. From Fig. 6.4, it can be observed that the nature of the curve for both $CO_2$ and CO mass flow rate tends to be asymptotic at the higher oxygen concentration. With an increase in oxygen concentration, the formation of $CO_2$ is promoted. In contrast, the formation of CO is suppressed due to the availability of excess oxygen on the carbon surface, which promotes complete combustion.

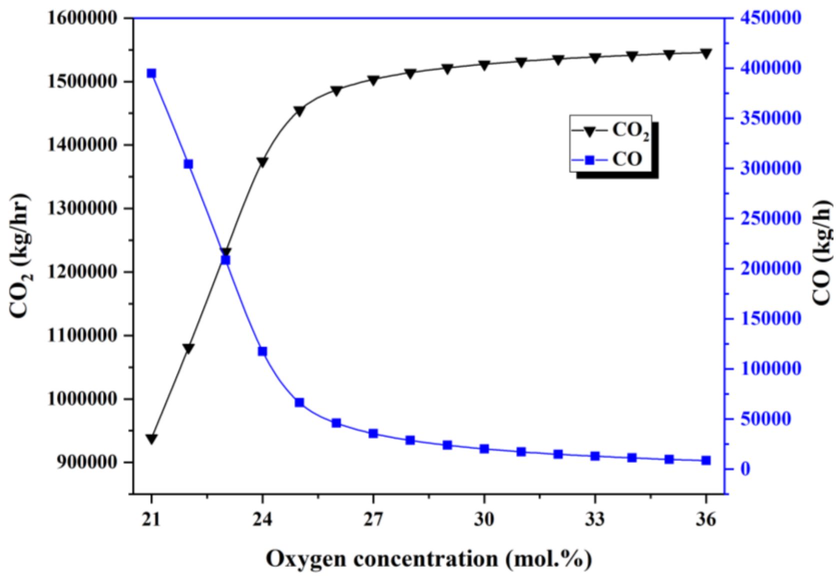


**Fig. 6.4.** Influence of oxygen concentration on the $CO_2$ and CO produced in the flue gas (RR=0.7)

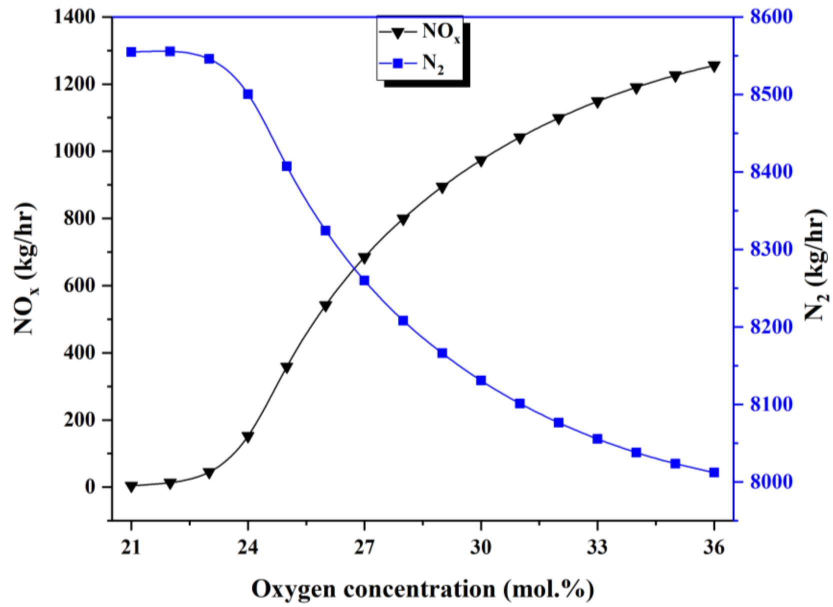


**Fig. 6.5.** Influence of oxygen concentration on the $NO_x$ and $N_2$ produced in the flue gas (RR=0.7)

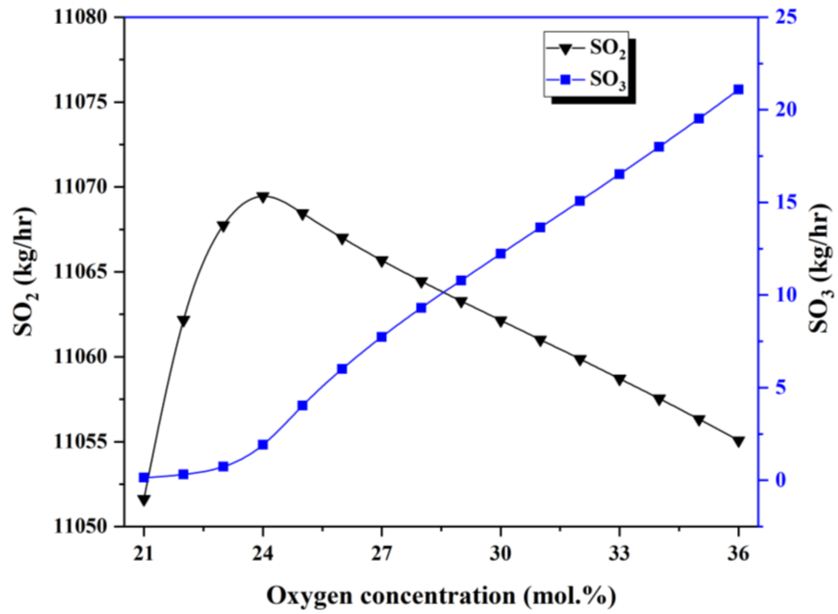


**Fig. 6.6.** Influence of oxygen concentration on the $SO_2$ and $SO_3$ produced in the flue gas (RR=0.7)

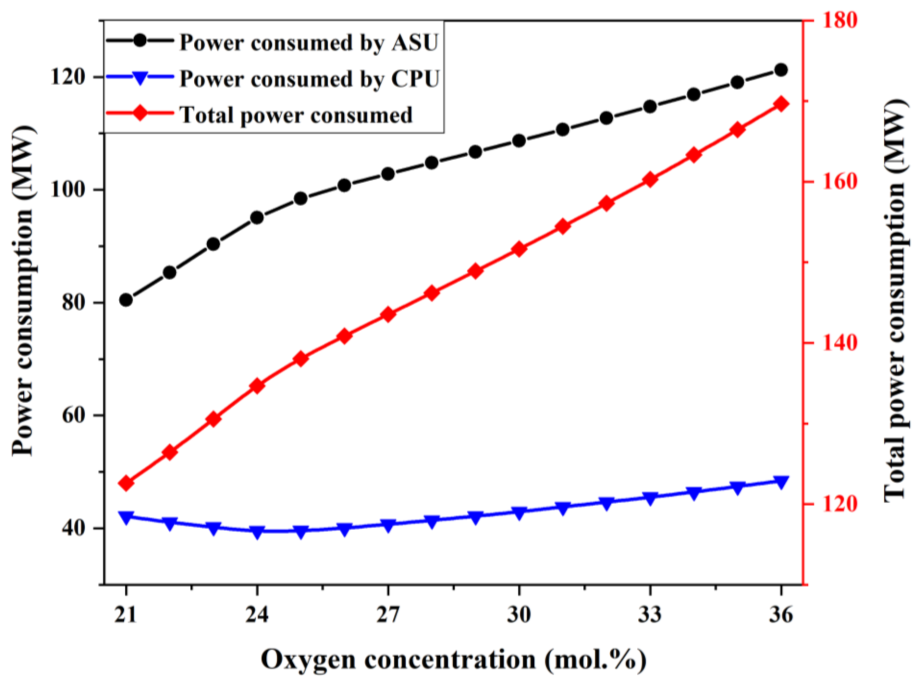


**Fig. 6.7.** Influence of oxygen concentration on the power consumption of ASU, CPU and total power consumption (RR=0.7)

Fig. 6.5 shows that the $NO_x$ formation is enhanced with an increase in oxygen concentration in the oxidizer. The formation of thermal and prompt $NO_x$ has been reduced to almost zero under oxy-coal combustion atmosphere due to replacement of air (the nitrogen present in the air contribute to thermal and prompt $NO_x$) with the mixture of oxygen and recycled flue gas (RFG). Under oxy-coal combustion, only fuel $NO_x$ has a considerable contribution to the total $NO_x$ produced (Jin et al., 2015b). With an increase in the concentration of oxygen, the conversion of $NH_3$ and HCN into $NO_x$ has been enhanced, which increased total $NO_x$ concentration.

Fig. 6.6 displays that the amount of both $SO_2$ and $SO_3$ increase up to oxygen concentration 24%, after that amount of $SO_2$ in flue gas tends to decrease, whereas amount of $SO_3$ increases. At oxygen concentration beyond 24%, some amount of $SO_2$ is easily oxidized to $SO_3$ due to the presence of higher concentration of oxygen. That's why the concentration of $SO_2$ in flue gases tends to decrease at higher oxygen concentration.

Fig. 6.7 shows the influence of the concentration of oxygen on the power consumption of ASU, CPU and total power consumption. It can easily be observed that the increase in oxygen concentration has affected power consumption of ASU and CPU. The increase in the concentration of oxygen has a more pronounced influence on ASU power consumption than the CPU power consumption. Increase in oxygen concentration from 21% to 36%, has increased the power consumption of ASU and CPU by 51% and 15% respectively. To increase the oxygen concentration in oxidizer, the amount of air supplied to ASU increases, that is the primary cause of the increase in power consumption of ASU. As recycle ratio of 0.7 is maintained while increasing the oxygen concentration, only 30% of flue gas produced is flown through the CPU. That's why the power consumption of CPU is not much affected with an increase in oxygen concentration.

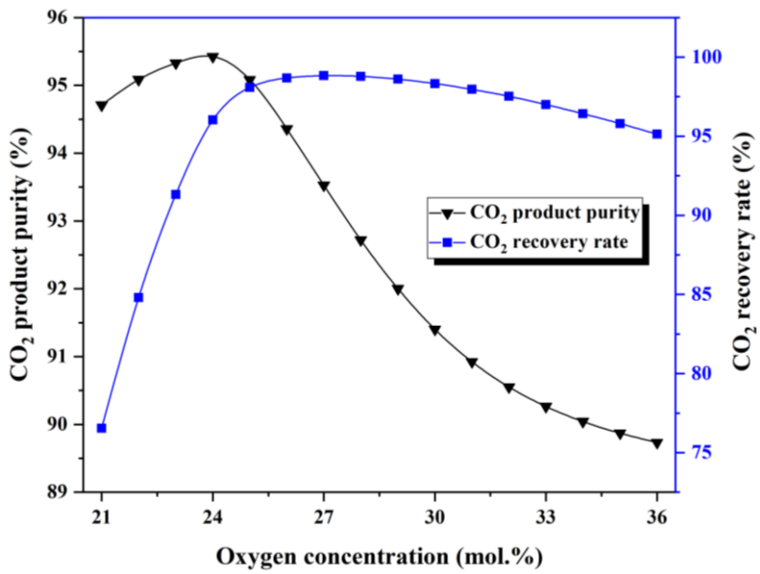


**Fig. 6.8.** Influence of oxygen concentration on the $CO_2$ product purity and $CO_2$ recovery rate (RR=0.7)

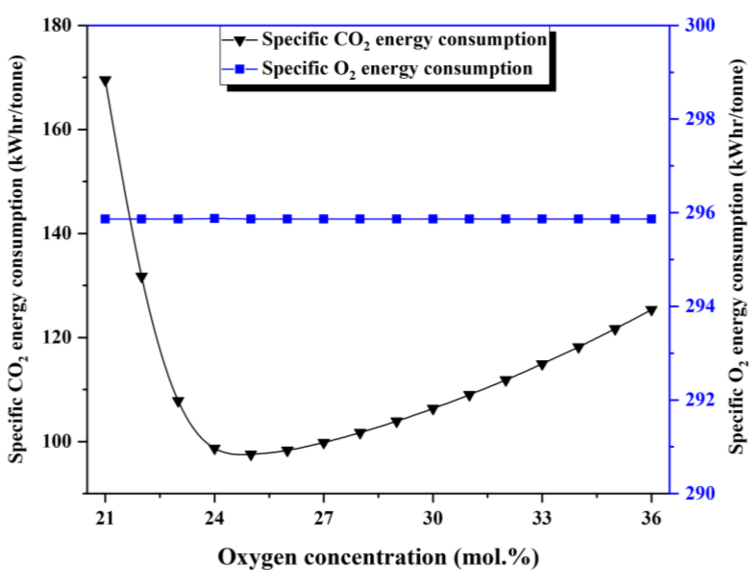


**Fig. 6.9.** Influence of oxygen concentration on the Specific energy consumptions of $CO_2$ and $O_2$ (RR=0.7)

Fig. 6.8 shows the influence of the oxygen concentration in the oxidizer on the $CO_2$ product purity and $CO_2$ recovery rate obtained after the CPU unit. Initially with an increase in oxygen concentration, $CO_2$ product purity rises, reaches its maximum value at oxygen concentration of 24%. The further increase in oxygen concentration diminishes the $CO_2$ purity obtained after CPU. The oxygen concentration of 36% produced $CO_2$ purity of around 90% only. $CO_2$ recovery rate rises sharply with the increase in oxygen concentration. Increase in oxygen concentration beyond 25% has less influence on $CO_2$ recovery rate. At oxygen concentration of 25%, the optimum values of both $CO_2$ purity and $CO_2$ recovery rate can be observed.

Fig. 6.9 displays the influence of the concentration of oxygen in the oxidizer on the specific energy consumption of $CO_2$ and $O_2$. At oxygen concentration of 21%, the specific energy consumption was very high (around 170 kW.hr/tonne $CO_2$). With an increase in oxygen concentration, specific energy consumption reduces. The oxygen concentration of 25%, has a specific energy consumption of 100 kW.hr/tonne $CO_2$. Further increase in oxygen concentration, the specific energy consumption rises slowly. The oxygen concentration of 36% has 122 kW.hr/tonne $CO_2$ energy consumption. Specific energy consumption of $O_2$ is independent on the amount of oxygen concentration in the oxidizer. The value of specific energy consumption for $O_2$ is constant at 295.85 kW.hr/tonne $O_2$.

### 6.10.2 Influence of Recycle Ratio (RR)

This section insight the influence of recycle ratio (RR) on the composition of flue gas produced under oxy-coal combustion atmosphere. Recycle ratio (RR) is defined as the ratio of the mass flow rate of recycled flue gas to the mass flow rate of total flue gas produced. To access the influence of recycle ratio (RR), the oxygen concentration is fixed at 25% by using the design specification block.

Fig. 6.10-6.12 displays the influence of RR on the composition of flue gas produced in oxy-coal combustion atmosphere. With an increase in RR, the formation of $CO_2$, $NO_x$, $N_2$, $SO_2$ and $SO_3$ is promoted, whereas the formation of CO is suppressed. As flue gas produced under oxy-coal combustion atmosphere has the highest amount of $CO_2$, with an increase in recycle ratio (RR), more $CO_2$ is supplied in oxidizer. That's why amount of $CO_2$ increases and CO decreases in the flue gas. Increase of recycle ratio from 0.7 to 0.75 increases $NO_x$ flow rate from 358 kg/hr to 634 kg/hr. Increasing recycle ratio (RR) increases the formation of $SO_2$ and $SO_3$.

Fig. 6.13 displays the influence of recycle ratio (RR) on the $CO_2$ product purity and $CO_2$ recovery rate obtained at the outlet of CPU. $CO_2$ product purity diminishes with the increase in recycle ratio. $CO_2$ recovery rate rises initially with an increase in RR, reaches its maximum value at RR 0.715. $CO_2$ recovery rate starts decreasing with an increase in RR beyond RR 0.715. Both $CO_2$ product purity and $CO_2$ recovery rate have their lowest values at RR 0.75.

Fig. 6.14 shows the influence of recycle ratio (RR) on the specific energy consumption of $CO_2$ and $O_2$ at a fixed $O_2$ content of 25 vol % in the oxidizer at the inlet to the furnace. RR

0.71 has the lowest specific $CO_2$ energy consumption, and RR 0.75 has the largest $CO_2$ energy consumption. Specific $O_2$ energy consumption is independent of RR.

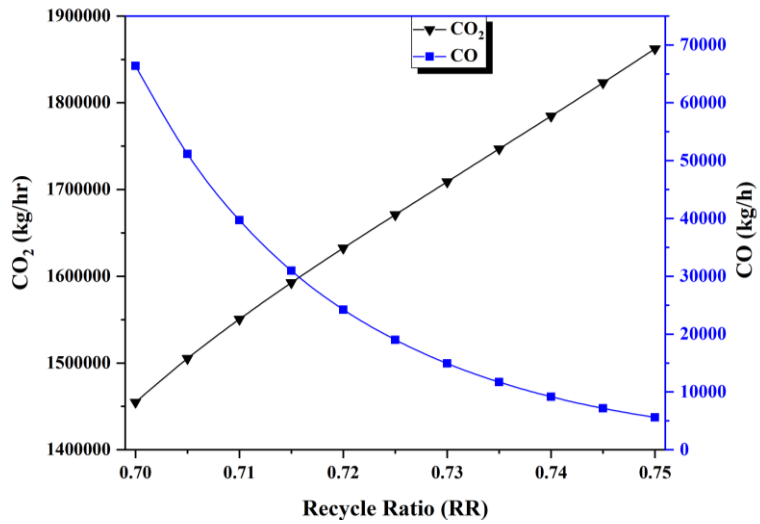


**Fig. 6.10.** Influence of recycle ratio (RR) on the $CO_2$ and CO produced in the flue gas (25 mol % $O_2$)

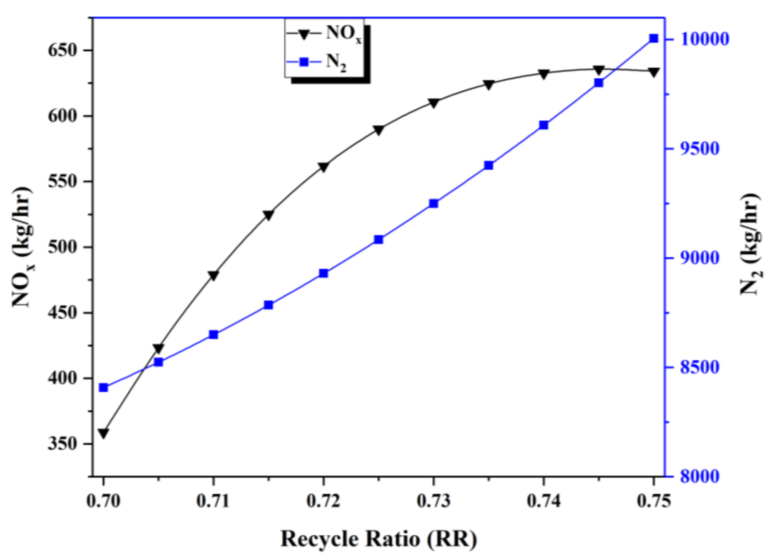


**Fig. 6.11.** Influence of recycle ratio (RR) on the $NO_x$ and $N_2$ produced in the flue gas (25 mol % $O_2$)

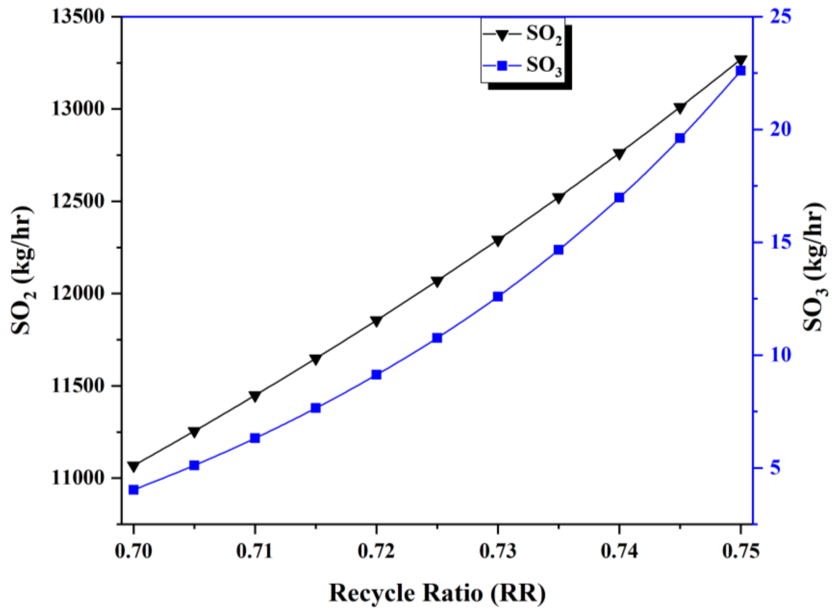


**Fig. 6.12.** Influence of recycle ratio (RR) on the $SO_2$ and $SO_3$ produced in the flue gas (25 mol % $O_2$)

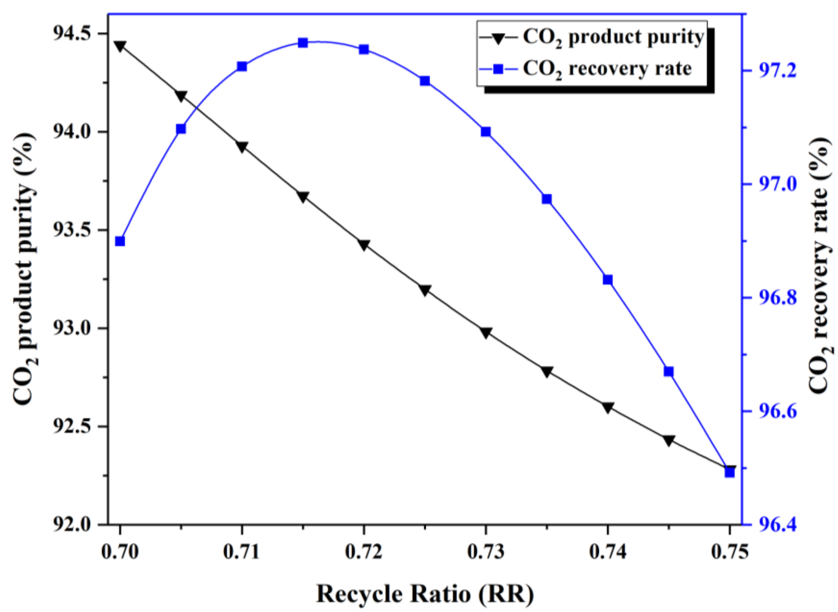


**Fig. 6.13.** Influence of recycle ratio (RR) on the $CO_2$ product purity and $CO_2$ recovery rate (25 mol % $O_2$)

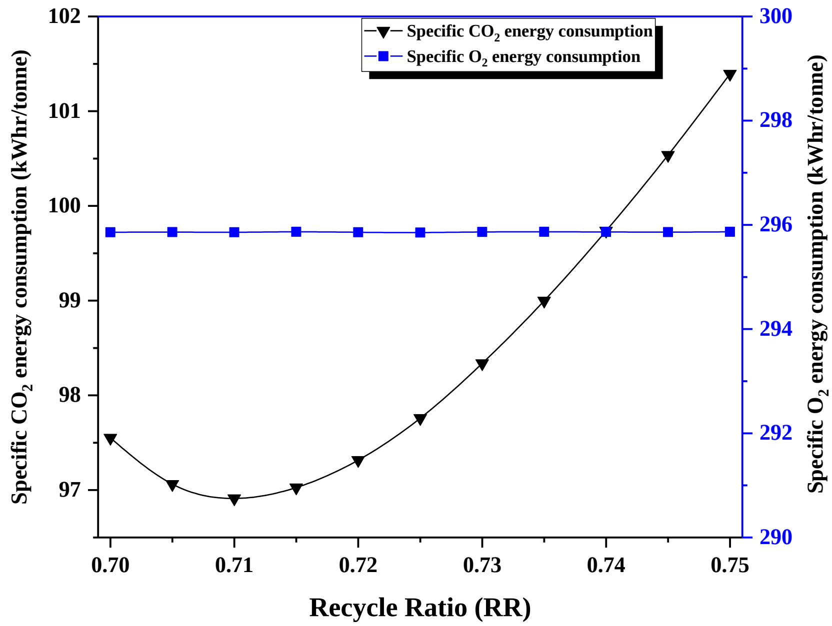


**Fig. 6.14.** Influence of recycle ratio (RR) on the Specific energy consumptions of $CO_2$ and $O_2$ (25 mol % $O_2$)

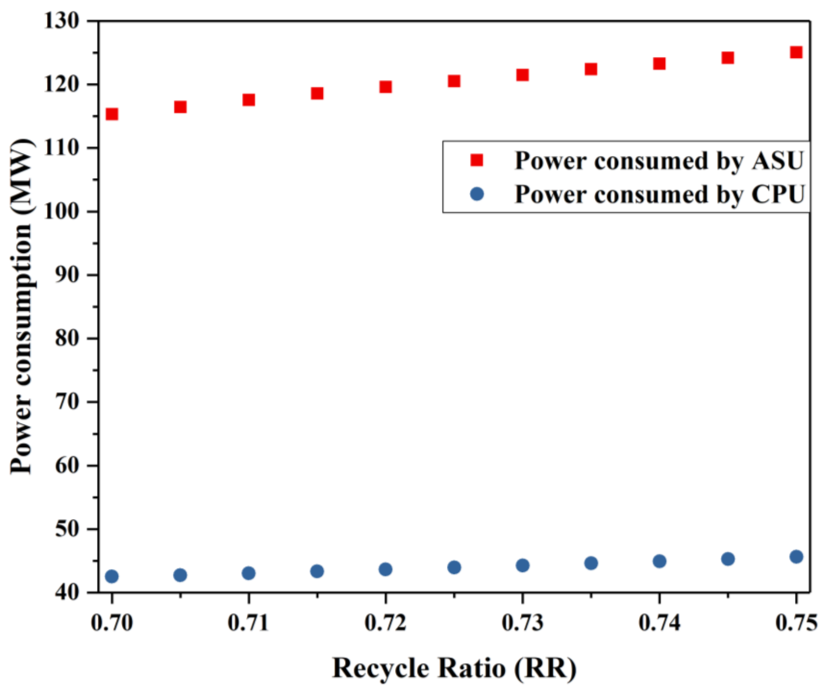


**Fig. 6.15.** Influence of recycle ratio (RR) on the power consumption of ASU and CPU

Fig. 6.15 shows the sensitivity analysis of the RR on the power consumptions of both ASU and CPU. With an increase in recycle ratio, the power consumption of both ASU and CPU rises gradually. As RR increases, the flue gas supplied at the inlet of the combustion chamber increases. To maintain constant oxygen concentration at that point, ASU has to increase the amount of oxygen slightly, that is the major cause of the increase in ASU power consumption. With an increase in RR, the production of flue gas rises, which in turn results in slightly more flue gas supplied to CPU. Due to the rise in the amount of flue gases at CPU inlet, the power consumption of CPU rises slightly.

### 6.10.3 Influence of oxygen purity

The sensitivity analysis of $O_2$ purity produced by air separation unit (ASU) on the mole fraction of $O_2$ supplied for combustion (S-11), and mole fractions of $O_2$ and $CO_2$ entering to the CPU unit (S-21) along with the power consumption (MW) of CPU have been studied in this section. The range of $O_2$ concentration from ASU has been set to be 0.95-0.98 at a step size of 0.05. Fig. 6.16 shows influence $O_2$ concentration from ASU on the optimal recycle ratio and CPU power consumption. The mole fraction of $O_2$ supplied for combustion (S-11) has been fixed at 25% in the mixture of $O_2$ and recycled flue gas (RFG) by changing recycle ratio (RR). From Fig. 6.16, it can be seen that $O_2$ concentration range of 95-98% has varied optimal recycle ratio from 0.7-0.709 and CPU power consumption from 51.1-48.1 MW.

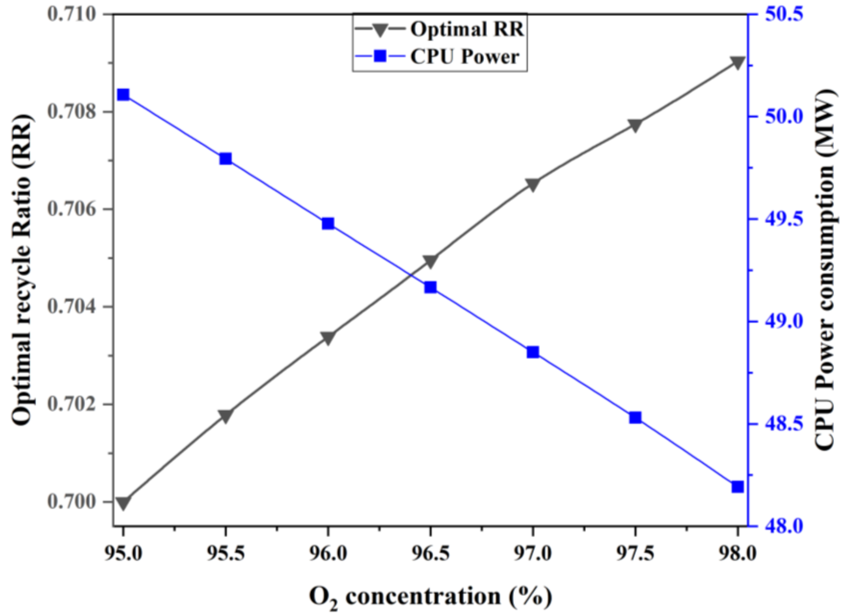


**Fig. 6.16.** Variation of optimal recycle ratio (RR) and CPU power consumption corresponding to the different $O_2$ concentrations from ASU

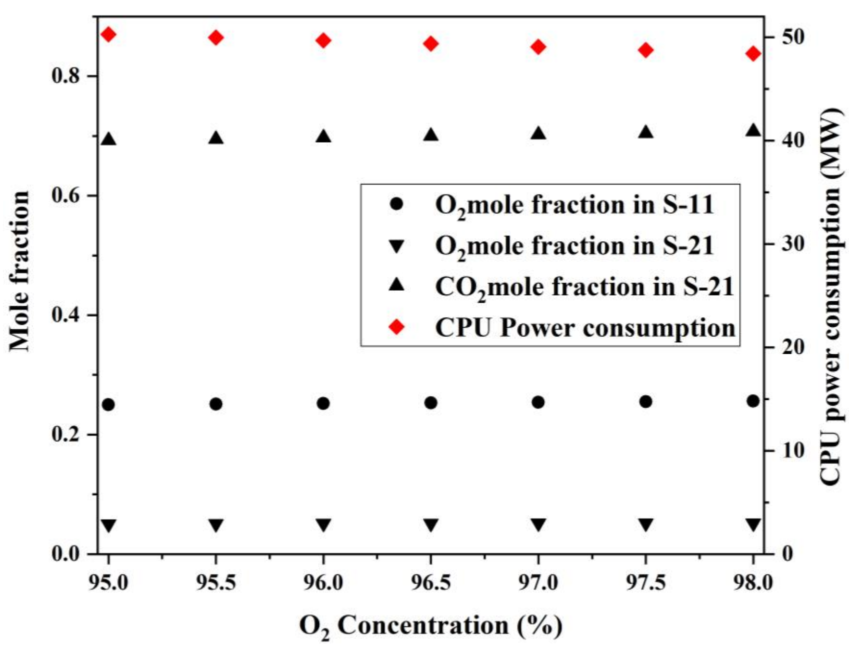


**Fig. 6.17.** Sensitivity analysis for the different $O_2$ concentrations from ASU

Effect of $O_2$ concentration from ASU on the mole fraction of $O_2$ supplied for combustion (S-11), and mole fractions of $O_2$ and $CO_2$ entering to the CPU unit (S-21) along with the power consumption (MW) of CPU at fixed recycle ratio (RR) of 0.7 have been shown in Fig. 6.17. Varying the $O_2$ concentration produced by ASU from 95-98% has changed the mole fraction of $O_2$ in S-11 by 0-2.4%, $O_2$ in S-21 by 0-2.6% and $CO_2$ in S-21 by 0-2.11%, respectively. The CPU power consumption has also been reduced by 0-3.72% points for $O_2$ concentration range of 95-98% from ASU. Thus, based on the above sensitivity analysis, it can be concluded that the $O_2$ concentration of 95% is well enough for the oxy-fuel combustion-based power generation. To produce higher $O_2$ concentration requires both the higher capital investment and more auxiliary power consumption. Although the power consumption of CPU is declining slightly, the power consumptions in different units and instalments are needed to be computed together to estimate the actual power consumption. However, these computations are beyond the scope of this work.

## 6.11 Environmental interaction

Environmental interaction of both conventional air-fired and oxy-fired supercritical power plant, describing the main streams into and out of the system is displayed in Fig. 6.18 and Fig. 6.19 respectively. From Fig. 6.18, it can be seen that the flue gas produced by the combustion of 102.9 kg/s of coal under the base case of conventional air fired combustion has the highest content of $N_2$, which amounts to be 480 kg/s. The conventional air-fired case has released 128.129 kg/s of $CO_2$ having mole fraction of 13.15% along with 1.15 kg/s CO, 2.35 kg/s NO and 0.93 kg/s $SO_2$.

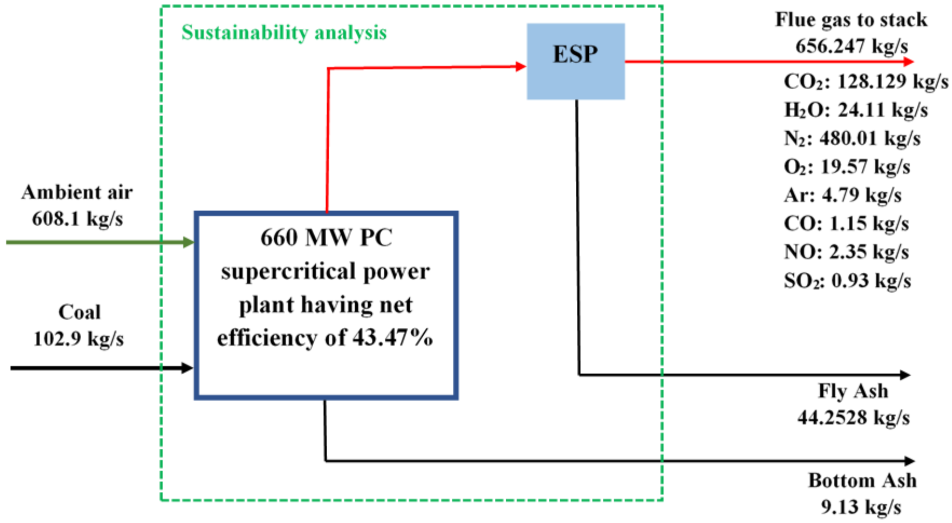


**Fig. 6.18.** Schematic of environmental interaction of conventional air-fired supercritical power plant

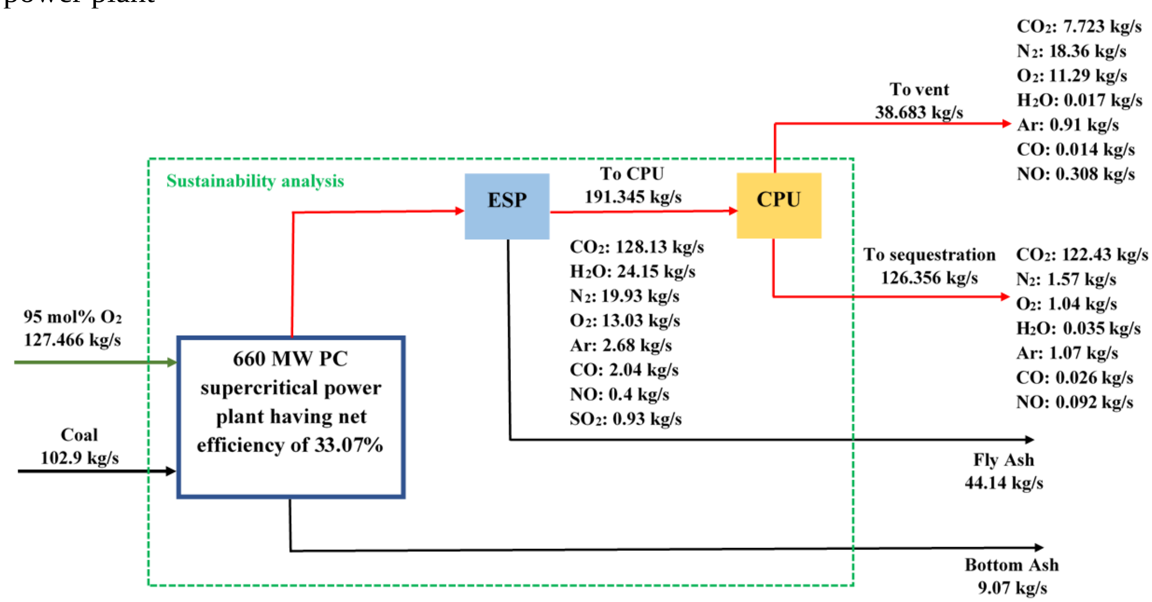


**Fig. 6.19.** Schematic of environmental interaction of oxy-fired supercritical power plant

On the other hand, oxy-fuel combustion-based supercritical power generation case has produced the highest amount of $CO_2$ in the flue gas. From Fig. 6.19, it can be seen that flue gas supplied to CPU and obtained after CPU for sequestration has 70% and 92% $CO_2$, respectively. In the oxy-fuel combustion-based supercritical power generation case, $CO_2$ concentration has been enriched to around 95% by flashing flue gas by the low temperature circuit. The small amount of $CO_2$ (7.72 kg/s) escaping with the gas phase has been vented into the atmosphere. From the analysis, it has been found that the around 94 mass % of $CO_2$ produced during combustion can be captured.

## 6.12 Summary

As a closure, in this chapter the oxy-fuel combustion concept has been implemented on 660 MW supercritical power plant to investigate the influence of important operating parameters on operational characteristics. It has been found in previous chapters that the oxy-coal combustion has flame stability issues at lower oxygen concentration. The combustion characteristics such as temperature and radiative heat transfer in oxy-coal combustion comparable to conventional air-fired combustion atmosphere can be obtained by increasing oxygen concentration. Thus, the basic understanding of oxy-coal combustion from previous chapters helped in the 0 D thermodynamic model prediction while investing the influence of oxygen concentration and recycle ratio on the performance of 660 MW supercritical power plant under oxy-coal combustion atmosphere in this chapter.

The excellent performance of oxy-coal combustion power plant has been observed in this chapter in term of its ability to capture carbon dioxide with 95% purity and 96% recovery rate. Based on the discussions held in this chapter, it can be concluded that the 10.4% reduction in net efficiency due to incorporation of energy consuming ASU and CPU units is acceptable as the prime objective of oxy-fuel combustion is to reduce the greenhouse gases emission. From the environmental interaction shown in this chapter, it has been found that the $CO_2$ content in the flue gas was 14.58% and 70% under air-fired combustion case and oxy-coal combustion case, respectively.